

# Comparative transcriptome analysis revealed the conversions of stamens into pistil-like structures in *Aegilops crassa* cytoplasmic male sterile wheat (*Triticum aestivum*)

Qi Liu

Northwest Agriculture and Forestry University

Zi han Liu

Northwest Agriculture and Forestry University

Wei Li

Northwest Agriculture and Forestry University

Xi Yue Song (✉ [songxiyue@nwafu.edu.cn](mailto:songxiyue@nwafu.edu.cn))

---

## Research article

**Keywords:** anther transcriptome; cytoplasmic male sterility; hybrid wheat; pistil-like

**Posted Date:** July 31st, 2019

**DOI:** <https://doi.org/10.21203/rs.2.12169/v1>

**License:** © ⓘ This work is licensed under a Creative Commons Attribution 4.0 International License.

[Read Full License](#)

---

**Version of Record:** A version of this preprint was published on February 4th, 2020. See the published version at <https://doi.org/10.1186/s12864-020-6450-2>.

# Abstract

Background: *Aegilops crassa* cytoplasm is an essential material for investigating the cytoplasm of cytoplasmic male sterility (CMS). Moreover, the stamens of C303A exhibit a high degree of pistillody, turning almost white. However, the underlying molecular mechanism of C303A pistillody remains unclear. Therefore, to gain a better understanding of C303A, the phenotypic and cytological features of C303A were observed to identify the key stage that the homeotic transformation of stamens into pistil-like structures, transcriptome profiles were determined by Illumina RNA sequencing technology (RNA-Seq) of stamen. Results: Through morphological observation, for CMS wheat with *Aegilops crassa* cytoplasm (CMS-C) line C303A, the pistil of which developed normally, but stamens were ultimately aborted and the stamens released no pollen when mature. According to the results of the paraffin section, stamens began to transform into pistils or pistil-like structures at binucleate stage (BNS). Therefore, the stamens of line C303A and its maintainer 303B at BNS were collected for transcriptome sequencing. A total of 20,444 wheat genes were detected as being differentially expressed between C303A and 303B stamens, included 10,283 up-regulated and 10,161 down-regulated genes. Gene Ontology Enrichment Analyses showed that most differentially expressed genes (DEGs) distributed on the metabolic process, cell, cellular process, catalytic activity and cell part. From KEGG, we knew that DEGs were mainly enriched to energy metabolism. We also found several essential genes that may contribute to pistillody in C303A. Based on the above analysis, we believe that due to the confusion of energy metabolism and reactive oxygen metabolism, thereby inducing the pistillody and eventually lead to the abortion of C303A. Conclusion: This study unravels the complex transcriptome profiles in C303A stamen, highlighting the energy metabolism and class B MADS-box genes related to pistillody. This work should lay the foundations of future studies in the mechanical response to wheat stamen and pollen development in CMS.

## Background

As a staple food for 35% of the world's population [1], wheat was the second largest staple food crop after rice and cultivated around 220 million hectares worldwide [2]. China was the largest producer and consumer of wheat around the world, with a cultivation area of about 24 million ha, an average yield of 4762 kg ha<sup>-1</sup>. Many significant challenges are facing in China, such as the increasing population and the reducing arable land area. Therefore, improving grain yield was an inevitable requirement to ensure food security. Therefore, improving grain yield was an inevitable requirement to ensure food security [3]. Overall, increasing wheat yield was a long-term goal of wheat breeding. And, utilization heterosis was a best method to increase yield and meet global food safety needs, such as maize, rape, sunflower, rice and sorghum [4]. Moreover, male sterility plants provide crucial breeding tools to harness hybrid vigor, or heterosis, in hybrid crops and also provide valuable material to study stamen and pollen development and nuclear-cytoplasmic interactions [5]. *Aegilops crassa* cytoplasm is the vital source of the cytoplasm of cytoplasmic male sterility (CMS), which had no harmful effect on the agronomic characters of common wheat. C303A that conferred by the cytoplasm from *Ae. Crassa*, was an outstanding wheat germplasm resources in cytoplasmic male sterility. But there was a fatal flaw on C303A, just like complex

restoration of fertility, poor outcrossing amount of wheat and fewer restorer lines. Due to these reasons, C303A was hard to use its heterosis but had great research potential as an extensive germplasm resource. For example, the stamens of C303A exhibit a high degree of pistillody, turning almost white because of the nuclear-cytoplasmic interaction when compared with its maintainer line 303B. In novel studies discovered an alloplasmic line of Norin 26 (N26) with *Ae. crassa* cytoplasm, which showed male sterility under long-day conditions (>15 h light period) because of pistillody [6]. So, we might assume that some factors in the *Ae. crassa* cytoplasm provoked pistillody, probably mitochondrial gene (s) [7]. However, studies on the pistillody identity in wheat are still superficial. C303A is a significant material for studying the pistillody of wheat. Therefore, this study describes some characteristics of C303A, including its floret morphology, cytological mechanism, physiological index, and molecular mechanism. The analysis of mutations *Arabidopsis thaliana* and *Antirrhinum majus* has allowed the formulation of the ABC model of flower organ [8]. Subsequent studies analyzing orthologs of the MADS-box genes have provided novel insights into the ABC mechanisms, so a landmark accomplishment in plant developmental biology that is the ABCDE model of flower organ identity [9, 10]. In this model, classes B, C, and E specify stamens class C and E genes define carpels, and class D and E genes determine ovule. Currently, the MADS-box gene that has cloned in wheat includes thirteen MIKC c-type MADS-box subfamily genes. From (cr)-CSdt7BS isolated two PISTILLATA (PI)-type class-B MADS-box genes, WPI2 and WPI1, and supposed that alterations caused pistillody in (cr)-CSdt7BS wheat to the expression pattern of class-B MADS-box genes [11]. Moreover, loss of function of class B MADS-box genes leads to pistillody in *Arabidopsis* [12] and *Antirrhinum* [13]. Therefore, wheat class B MADS-box genes could be related to the induction of pistillody in wheat. At present, the molecular mechanism of stamen development and nuclear-cytoplasmic interactions were clearly explained in *Arabidopsis thaliana*, rice, maize and other model plants, but it is rarely studied in non-model plants. Wheat is a heterologous hexaploid plant with a complex genetic background, and it is inefficient and difficult to study a great quantity of genes involved in the stamen development and nuclear-cytoplasmic interactions network by traditional molecular biology methods. Therefore, high-throughput transcriptome sequencing (RNA-Seq) provides comprehensive and rapid access to almost all transcript information in wheat stamen during binucleate stage. So, it is easy to systematically analyze the DEGs which related to pistillody. Our research carried out RNA-Seq on the stamen of C303A and its maintainer line 303B and presented herein focused on the discovery of metabolic processes and transcription factors contributing to pistillody in C303A. A comprehensive understanding of the genetic network changes and expression patterns of C303A pistillody will enable the future utilization of molecular mechanism in stamen development and nuclear-cytoplasmic interactions.

## Results

### Phenotypic Characteristics of C303A and 303B stamen

The wheat CMS line C303A was developed from stable sterile lines by consecutive backcrossing with 303B, as the donor parent, over 20 times in Yangling, China. To get the abortive morphological feature of C303A, we collected from C303A stamens in five developmental stages. Field comparative observation

showed that except for floral organs, there was no significant diversity in growth and overall morphology between the CMS line C303A and its isomaintainer line (303B) (Fig. 1). At BNS, the anthers of 303B were quite full and yellowish, and which was bright yellow and the upper and lower ends were bifurcated, normal cracking accompanied by a large number of pollination phenomenon at the trinucleate stage. However, the anther color of C303A was white in the tetrad stage. Stamen malformations occurred in uninucleate stage and individual stamens with curved folds. Some stamens have become a combination of stamens and pistils at the binuclear stage. The stamens at the trinucleate stage have been completely transformed into pistils (Fig. 2). Moreover, to accurately observe the cytological structure of pistillody stamens, we used paraffin section. As shown in Figure 3, there were apparent differences between fertile stamen and pistillody stamen. Compared with the tetrad stage of 303B, the four anther locules in C303A sequentially shrunk and shriveled. Meanwhile, there was a marked degradation in one anther locule without microspores, another anther locules were empty and only with a very thin tapetum. However, a small number of microspores were detected in the other two anther locules. At early uninucleate stage, the degradation anther locules have been increased. Besides, the microspores shrank and condensed obviously in another anther locule. During the later uninucleate stage, the outlines of the tapetal cell and microspores were wholly invisible and some vascular bundles were found on degradation anther locule, thereby contributing to transport of nutrients to the locule for ovule formation. At the binucleate stage, the two degenerated chambers began to merge, and we speculate that this may be the beginning of the formation of ovules. Up to the trinucleate stage, the structure of the ovule in the pistillody stamen was determined in transverse and longitudinal sections. The above results indicate that the pistillody stamens contained ovule structures, instead of pollen grains and tapetum, thereby the stamens of C303A are unable to produce mature pollen grains, which could be detected by potassium iodide staining. So, we deduced that pistillody might occur at the binucleate stage.

### **Sequence Analysis Using RNA-Seq**

To understand the basic molecular mechanism responsible for the pistillody at the transcriptional level, we conducted employing an Illumina HiSeq PE1500 sequencer for a transcriptome sequencing analysis of binucleate stage stamen of CMS line C303A and its maintainer line 303B. Stamens were collected three times, for a total of three biological replicates and sequencing reads were 150 bp in length. After filtering out the reads with >10% ambiguous nucleotide, adapter sequences and low-quality regions, 270,683,956 clean reads were produced, with 131,000,548 reads from the maintainer line, and 139,683,408 from the CMS line. Additionally, the GC content ranged from 55.80% to 59.63% and the Q20 percentage surpassed 88.93%. Each sample's clean reads were matched to *Triticum aestivum* reference sequence, where the alignment efficiency was between 60.46% and 68.09% (Table 1). The throughput and sequencing quality show that the RNA-Seq data we obtained were adequately high quality to ensure further analysis.

### **Identification of DEGs by RNA-Seq**

In total, RNA-Seq detected 179,898 genes. For determining the significant difference in gene expression levels, we used the  $FDR < 0.05$  and  $\log_2$  Fold Change ( $|\log_2 FC| > 1$ ) as the threshold. To compare the DGEs at the binucleate stage for C303A and 303B based on significant differences (Fig. 4). A total of 20,444 genes were discovered as being differentially expressed between C303A and 303B stamen. These DEGs included 10,283 up-regulated and 10,161 down-regulated genes in the C303A stamen compared with the corresponding expression levels in the 303B stamen.

### Gene Ontology Enrichment Analyses of the DEGs

GO is a universal standardized gene functional classification system that gives a dynamically-updated controlled vocabulary and a rigidly defined concept to comprehensively describe properties of genes and their products in any organism [14]. After enrichment analysis, the DEGs found in C303A have been annotated 36 functional groups (Fig. 5). Among the biological process functions, the central DGEs were associated with cellular processes, single-organism process, localization and metabolic processes function. With respect to the cellular component, the DGEs associated with cell, cell parts, membranes, and organelles. Besides, binding, catalytic activity and transporter activity are closely related to molecular function. There are twenty significantly enriched GO terms in the biological process functions which revealed by hypergeometric tests. Among twenty GO terms (Table S1), there are two terms the q-value equals zero: (GO: 0005975) carbohydrate metabolic process and (GO: 0044710) single-organism metabolic process. The DEGs in different functional categories may provide a valuable resource for the study of stamen development in C303A.

To identify biological pathways, the DEGs in the binucleate stage were mapped to 129 pathways in the KEGG database, where the top 36 pathways (Table S2) were deemed significant at a cut-off FDR corrected q-value  $< 0.05$ . And the main DEGs mainly comprised starch and sucrose metabolism, amino sugar and nucleotide sugar metabolism, glycolysis, phenylpropanoid biosynthesis, pyruvate metabolism, citrate cycle (TCA cycle), pentose and glucuronate interconversions and cyanoamino acid metabolism (Fig. 6). Most of the genes mapped in the nine significantly enriched pathways had down-regulated expression trends except for the circadian and phenylpropanoid biosynthesis. Indicating that starch and sucrose metabolism, glycolysis and TCA cycle could be essential for pollen development. Previous studies have proved that the TCA cycle has a pivotal role in plant male sterility [15] and the normal energy metabolism process of plants can satisfy their growth and development. So, we pay more attention to the significant genes related to these pathways, which may explain why no microspores in pistillody stamen.

### Identification of MADS-box transcription factor involved in pistillody

In plant, the MADS-box gene family play essential role in the ABCDE model of flowering. According to this mole, 3 (*TaAGL40*, *WM19B*, and *WM9B*), 1 (*WM27A*), 2 (*WM24A*, *TaAGL36*) and 5 (*TaAGL14*, *WM25*, *MAD-Box factor 2A*, *MAD-Box factor 2D*, and *MAD-Box factor 2B*) wheat genes were identified to be class A, class D, SVP and class B, respectively (Fig. 7). Meanwhile, previous studies have identified several class B MADS-box genes in wheat, such as *WPI2* and *WPI1*. These genes are mainly related to the transformation of wheat from vegetative growth to reproductive growth. These genes change their

expression patterns in heterogeneous wheat and common wheat, and which contribute to the transformation of their stamens into pistil-like structures. The conserved domains and motif compositions of class B MAD-box genes were analyzed. As shown in Figure 8, a conserved K-box is present in the most class B MAD-box genes, except for MAD-box factor 2 genes. A distinct MADS superfamily was exclusively found in *OsMADS32* and *TaAGL14*. From the analysis of motif compositions, there are 10 conservative motifs identified in class B MAD-Box, which are named motif1 to motif 10. Motif\_1, as a conservative motif of MAD-Box, appears in all MAD-boxes of Class B. Motif\_2 only appears in AP1 subfamily, motif\_10 only appears in GGM13 subfamily and motif-10 only appears in MAD-box factor transcription factor 2. Based on the above results, we find that WM25 and *OsMAD29*, *TaAGL14* and *OsMAD32* have the same conserved domains and motif compositions, which they might have the same functionality. Meanwhile, the results of amino acid sequence alignment showed that the similarity was more than 92% (Fig. s1, Fig. s2).

### **A Possible molecular basis for the energy deficiency model in C303A**

According to the analysis of the above results, we get three metabolic pathways involved in carbohydrate metabolism and energy metabolism (glycolysis, TCA cycle and pyruvate metabolism) to regulate pollen development. Combined with previous studies, we suggested a probable regulatory network leading to no microspores in C303A (Fig. 9). During anther and pollen development, the amount of pyruvate, the final product of glycolysis, might be decreased due to the down-regulated expression of the enzyme involved in glycolysis, which affects the TCA cycle to some extent. Also, the down-regulated expression of the enzyme genes associated with the TCA cycle contributed to a reduction in the number of coenzymes (FADH<sub>2</sub> and NADH), whereby decreasing coenzymes entering the electron transport chain. In the electron transport chain, the down-regulation of antioxidant enzymes and key complexes represses electron transfer, and then electrons directly transfer to molecular oxygen, which produces excess ROS. Besides, upregulation of the activities of the antioxidant enzyme, which ruins the balance of the antioxidant defense system. Because ROS cannot be eliminated adequately immediately, which increases the consumption of ATP and the production of H<sub>2</sub>O<sub>2</sub> and this might be finally causing no microspores in C303A.

### **Validation of key DEGs by Real-time Quantitative PCR (RT-qPCR)**

To validate the sequencing data and possible pathways, the transcriptional expression of fifteen key DEGs involved in energy metabolism and pistillody were further analyzed by qRT-PCR (Fig. 10). Although quantitative difference existed in the two methods, the tendencies were same. The difference in the gene expression level was reasonable because of different working principles. Overall, these results demonstrated that our sequencing results were accurate and reliable, and further confirmed possibility on pathways related to stamen and pollen development.

### **Analysis of DEGs in energy metabolism pathway and determination ATP content and related enzyme activity**

The DEGs were annotated and analyzed in KEGG pathway database to obtain the DEGs related to energy metabolism. Out of which 82 DEGs were annotated as NADH dehydrogenase, ATP synthase, Citrate synthase, Isocitrate dehydrogenase, 2-oxoglutarate dehydrogenase and Malate dehydrogenase in the energy synthesis pathway. Then heat map was used to analyze the expression level of DEGs in binuclear stage (Fig. 11). The results showed that the expression level of energy synthesis pathway genes was significantly down-regulated at the binuclear stage. To further confirm the accuracy of results described above, we measured the amount of ATP at the binucleate stage (Fig. 12). The energy metabolism-related enzymes genes were significantly lower in C303A than that of 303B presented a heat map in Figure 8. Because of the altered of energy metabolism-related enzymes genes in the C303A pistillody stamen, we considered that the ATP in the pistillody stamen was also lower when compared with 303B stamen. According to the assays, we found that the ATP content in C303A stamen was also significantly lower than that in 303B. So, from these results we hypothesized that these genes involved in energy metabolism are associated with C303A pistillody.

### **ROS assay and activities of antioxidant enzymes**

Compared with the physiological research of fertile wheat, the previous research results showed that sterile wheat higher accumulation of  $H_2O_2$  and MDA and had a higher  $O^{2-}$  generation rate [16, 17]. Thus, we determined the  $O^{2-}$  generation rate as well as the  $H_2O_2$  and MDA contents during all of the anther developmental stages (Fig. 13). The rate of ROS production was significantly higher in C303A than that of its maintainer line during all of the anther developmental stages. Also, the  $O^{2-}$ ,  $H_2O_2$  and MDA contents were continuously raised in C303A with peak values at the uninucleate stage, whereas the MDA contents peak in the trinucleate stage. Therefore, these results imply that excessive accumulation of ROS may lead to abnormal of tapetal cell in C303A stamens. Furthermore, we also measured the activities of antioxidant enzymes such as CAT, SOD and POD. The SOD and POD activity in C303A remained at a high level throughout the whole course of pollen development, while the CAT activity remained high in the pistillody stamen only from the tetrad stage to the later uninucleate stage. According to these outcomes, it is possible that upregulation of the activities of antioxidant enzyme also reflects the extreme accumulation of ROS in the C303A, which upsets the balance of the antioxidant defense system and finally could contribute to pistillody in C303A.

## **Discussion**

Wheat is an allohexaploid, which contained three genomes (A, B, and D), and its genome approximately 17G. The formation of common wheat involves three primitive ancestral species and two natural hybrids. *Triticum urartu*, *Aegilops speltoides*, *Aegilops tauschii* were the progenitor species genome of the wheat. Compared with rice, corn and other crops, wheat molecular basic research is still weak, and the genetic background is relatively poor. In recent years, RNA-Seq, which based on Illumina sequencing platform, has shown itself to be a reliable tool with an excellently diverse range of applications, from detailed

researches of biological processes at the cell type-specific level, to give penetrations into fundamental questions in plant biology on an evolutionary time scale.

In this study, we performed comprehensive RNA-seq analyses of the stamen from C303A and 303B at the binucleate stage. Furthermore, compared with 303B, we detected many DEGs that involved the process of carbohydrate and energy metabolism of stamen in C303A and numerous of these DGEs decreased at the binucleate stage. Overall, we could suggest that the decrease or non-expression of these DEGs due to pistillody. And these DEGS may result in insufficient cellular energy supply and abnormal starch synthesis, which also disturbs the balance of material and energy metabolism in stamens and eventually leads to no pollen grain.

### **Starch and sucrose metabolism affected stamen development**

The natural development of microspore cannot do without carbohydrates, starch, amino acids and protein [17]. During the process of conversion from sterility to fertility on YS type thermo-sensitive male sterile wheat line A3314, the contents of polysaccharide were significantly higher [18]. Starch, as the most common form of carbohydrate storage in cells, was the main source of energy metabolism in plants. In previous studies, the abortion of cotton nuclear male sterile anther showed that less starch accumulation in the male sterile line, which could conclude that anther abortion might be due to the disruption of soluble sugar transport or starch synthesis [19]. The growth and development of wheat stamen are closely associated with carbohydrate metabolism since carbohydrates provide energy for the development of wheat photosynthetic apparatus. Sucrose and starch were the main forms of carbohydrate and the metabolism of it was crucial to plant. It was a complex physiological process with dozens of enzymes involved. AGPase is the rate-limiting enzyme in starch synthesis, which reversibly catalyzes the substrate adenosine diphosphate glucose in the synthesis of starch. In monocots, AGPase consists of two large subunits (LS) and two small subunits (SS) that interact and polymerize into the native heterotetrameric enzyme structure [20, 21]. The small subunit (Su) is the catalytic center of enzyme activity and the key site of enzyme allosteric effect [22]. The two genes were encoded by different genes, while studies in *Arabidopsis* subbodies showed that they were functionally interdependent and lacked a single gene. In our research found that AGPase was decreased at the binucleate stage in C303A. Moreover, exopolygalacturonase and Alpha-glucan phosphorylase were involved in starch synthesis and accumulation, which activated the corresponding metabolic pathways to improve the accumulation and synthesis of starch. Thus, these results showed that starch and sucrose metabolism in C303A anther was probably weakened that in 303B anther, which was closely associated with no pollen in C303A.

### **DEGs involved in Energy Metabolism**

The normal energy metabolism process of plants can satisfy their growth and development. Energy metabolism mainly includes these major processes: such as photosynthesis, glycolysis, oxidative phosphorylation, and the TCA cycle. Energy metabolism process requires a lot of related genes or proteins to be adjusted together. A large number of investigations have revealed that the abnormal performance of these proteins or genes in stamen will inevitably interfere with the energy supply of pollen

development – for example, using the fluorescein-luciferase way to determine the content ATP of the anther, which found that the content of ATP in AS was much lower than that in normal anther from the early stage of pollen grains to maturation phase [23]. Similarly, Xia and Liu [24] used the same method to determine the ATP content of stamen at different developmental stages using the corn CMS line and its maintainer system. The results showed that the content of ATP of the sterile line was significantly lower than that of the maintainer in the anther, and it was considered that a large amount of energy was consumed during the pollen abortion process because the formation of microspores requires a large amount of energy and nutrients. In addition, the absence of microspores in C303A may be due to the down-regulation of energy metabolism in C303A during pistillody stamens formation. Moreover, Hexokinase-5, 6-phosphofructokinase 5 and pyruvate kinase played a vital role in the glycolysis pathway, which was significantly down-regulated in C303A. These genes may have an impact on the development of stamen. The down-regulation of these significant genes directly led to the number of respiratory substrates decreased and can also interfere with the electron transmit chain (ETC) on mitochondria. Also, many DEGs that related to ETC and TCA decreased in this stage and our examinations of the ATP contents also uphold this standpoint (Figure 12). So, we could suggest that the energy of C303A pistillody stamens was lower than that of 303B stamens, which can not meet the basic energy requirement of microspores in C303A. As a result, the pistillody stamens of C303A cannot form microspores.

### **DEGs Related to Pistillody**

When the stamen of flower showed the homeotic transformation of stamens into pistil-like structures, the phenomenon is called pistillody, which can cause stable and complete male sterility, and existed in some species, such as in *Arabidopsis* [25] and *Antirrhinum* [13, 26]. In present study, pistillody advents were occurred in CMS wheat line C303A with *Aegilops crassa* cytoplasm, but the pistillody phenomenon of C303A was not clear, so we used RNA-seq to elucidate the molecular mechanism of pistillody induction. Therefore, we selected some reported genes that affected flower development.

PI and AP3 proteins specifically bind together to implement the class-B function and to localize into the nucleus [27]. Moreover, according to the ABC model, class-B MADS-box genes are expressed in both whorl 3 and whorl 2 for identification of stamens and lodicules in *Arabidopsis* [25]. Previous studies showed that the pistillody emerged from a deficiency of WP11 gene expression in whorl 3 [28]. Furthermore, in monocots, a maize class-B gene-deficient mutant, *silky1*, displayed male sterility because of homeotic conversions of stamens into carpels [29] and transgenic rice expressing antisense RNA of the class-B gene *OsMADS4* showed alteration of stamens into a carpel-like organ [30]. So, pistillody was caused by changes in the expression pattern of class B MADS-box gene in wheat. In the present study, we find a paralogous gene (*TaAGL14*) may have an analogous role to *OsMADS32*. In the research of *cfo1-1*, the strong alleles of *OsMADS32*, discovered that the number of pistil was increased and *OsMADS32* was required for pistil development and floral meristem determinacy. Furthermore, in C303A gene *TaAGL14* was upregulated. Thus, class-B MAD-box genes may contribute to pistil development.

MIKC-type MADS-box transcription factor genes related to a range of critical developmental processes, such as ovule development, vegetative growth, flower morphogenesis and fruit formation [31, 32]. The MADS-box transcription factor, *WM27A*, the expression pattern was compatible with its function as the class D gene and regulated ovule identity specification on the basis of the “ABCDE” model in flower development [33]. Previous studies found that *WM27A* was deeply expressed in pistils and caryopses, with weak expression in stamens and extremely high expression during late spike development. Moreover, the phylogenetic tree of the Nucleotide sequences of a MADS-box transcription factor *TaMS-MADSbox* (GenBank accession number: 36925702) which linked to fertility conversion in male sterile wheat lines [34], along with MADS-box transcription factor from our sequencing data, showed that *WM27A* and *TaMS-MADSbox* in the same branch. In our study, *WM27A* expression was unregulated in C303A. Thereby, it is obvious to find that this result is very similar to the results of previous studies. EPIDERMAL PATTERNING FACTOR-LIKE (EPFL) family functions in various plant growth and development aspects, such as the guidance of inflorescence architecture and pedicel length. And in wheat *TaEPFL1* secreted peptide gene is essential for stamen development [35]. Moreover, *TaEPFL1* gene is expressed at an abnormally high level in pistillody stamens compared with that in pistils and stamens. In our study, we found that genes were coding the EPFL protein in C303A. On the whole, these results could speculate that these genes brought about pistillody. However, the mechanisms by which these genes control wheat stamen and pistil development remains to be widely explored.

## Conclusions

For CMS-C line C303A, the pistil of which developed normally, but stamens were ultimately aborted and the stamens released no pollen when mature. According to the results of the paraffin section, stamens began to transform into pistils or pistil-like structures at binucleate stage (BNS). And we employed RNA-Seq results showed that mainly via effects on carbohydrate and energy metabolism, and downregulating the expression of enzyme genes that involved in carbohydrate and energy metabolism, which were closely related to pollen development. Thus, we suggested a possible regulatory network and did deem that the downregulation of key genes in this regulatory network, which is the leading cause of no microspores in C303A. Besides, ATP, ROS and ROS scavenging enzymes were measured to confirm the regulatory network. Furthermore, the regulation of pollen and stamen development is affected by the MADS-box transcription factor families. The conversions of stamens into pistil-like structures in C303A due to the effects of multiple genes rather than a single gene. This work should lay the foundations of future studies in the mechanical response to wheat stamen and pollen development in CMS.

## Methods

### Plant Materials, Plant Growth, and Anther Collection

The CMS line C303A and its isomaintainer line 303B were employed in this research. All of the experimental materials were cultivated conventionally at the Northwest A&F University experimental station (Yangling, China). The pollen developmental stages, including tetrad stage (Tds), early

uninucleate stage (Euns), later uninucleate stage (Luns), binucleate stage (Bns), and trinucleate stage (Tns), were identified by acetic red dyeing methods. Because C303A had no microspore, we determined the developmental stage of C303A by observing the characteristics of 303B. And previous studies have shown that the spike development stages of 303B and C303A are the same [36]. Therefore, the average of the spike length and the external morphological characteristics of each period of 303B were determined. In the tetrad stage, the spike length of the 303B was 3.7 cm and the spike apical was in the middle of the second top leaves and the third top leaves. At the early uninucleate stage, the spike length of the 303B was 10.5 cm and the spike apical was in the middle of the second top leaves and the flag leaf. At the later uninucleate stage, the spike length of the 303B was 12.9 cm, and the awn was just wholly extracted. At the binucleate stage, the spike length of the 303B was 11.4 cm, and wheat earing was about 2/3. At the trinucleate stage, the spike length of the 303B was 14.5 cm and all spike have been pulled out, which also found some of glume opening and anther exposed. According to these characteristics of 303B, we collected different developmental flowers and stamen from materials for morphological and cytological observations during heading and anthesis. Moreover, the stamen at the binucleate stage were collected from three individual fertile plants (303B-1, 303B-2, 303B-3) and three individual sterile plants (C303A-1, C303A-2, C303A-3) for transcriptome sequencing, creating three biological replicates. The harvested stamens were quickly flash-frozen in liquid nitrogen and then stored at -80 °C for further investigated.

## **Morphological analysis**

Carefully peel the stamen and florets with tweezers and anatomical needles. The morphological characteristics of florets and stamen were observed and photographed under a microscope (Preiser Scientific, Louisville, KY, USA). Mature pollen grains were dipped in a drop of I<sub>2</sub>-KI solution. All of the samples were placed in FAA (Formalin-acetic acid-alcohol) fixative solution and stored in 4 °C refrigerators. The specimens were dehydrated through a graded ethanol series, infiltrated with xylene and then embedded in paraffin. The sections measuring 5 µm were placed onto gelation-coated glass slides (Sigma-Aldrich) and stained with toluidine blue [37]. The stamens of different stages were captured using a DS-U2 high-resolution camera mounted on a Nikon ECLIPSE E600 microscope (Nikon, Tokyo, Japan).

## **Total RNA extraction, cDNA library preparation and Illumina sequencing**

Total RNA was extracted into C303A and 303B stamen during BNS stage using Trizol reagent (Takara Biotechnology, Dalian, China). The integrity of total RNA was identified by 1% agarose gel electrophoresis, the sample OD260 and OD230 were detected by Nanodrop spectrophotometer, then the purity of RNA was analyzed, and the sample concentration, RIN value and 28S/18S value were determined by Agilent2100 bioanalyzer (Agilent Technologies, Santa Clara, CA, USA).

All samples were given to Sagene Biotech Co. Ltd (Guangzhou, China) for library and sequencing, and the eukaryotic mRNA was enriched with Oligo (dT) beads. And then the fragmentation buffer was used to interrupt the mRNA into short fragments to mRNA. cDNA is synthesized by using mRNA as a template by

using random primers. DNA polymerase I, RNase H, dNTP and buffer were added to synthesize Second-strand Then those were purified with QiaQuick PCR extraction kit (GeneStar Co. Ltd, Beijing, China). The purified cDNA was needed to end repaired, poly (A) added. Finally, PCR amplification was performed and the PCR product was purified with AMPure XP beads [Beckman Coulter, Brea, CA, USA] to obtain a final library. After the library is qualified, different libraries are pooled according to the requirements of the effective concentration and the target data volume, and then the Illumina HiSeq sequence is performed.

### **Raw data filtering and transcripts splicing**

The process of raw data filtering was as follows: (1) removing reads with adapter; (2) eliminating reads containing more than 10% of unknown nucleotides (N); (3) excluding low-quality reads. In order to ensure the quality of information analysis, raw reads were filtered to obtain clean reads, and subsequent analysis is based on clean reads.

Using Chinese spring (CS) as the reference genome (Ensembl release 31 IWGSC1.0 + NC\_002762.1), clean reads were compared to reference genome sequences by applying software HISAT2 (v2.2.0.4, <https://ccb.jhu.edu/software/hisat2/index.shtml>) [38], and the alignment was assembled using Cufflinks [39] (v2.1.1, (<http://cole-trapnell-lab.github.io/cufflinks/>)) software to construct the transcripts.

### **Screening and analysis of differential gene expression**

The input data of gene differential expression was read count data obtained in gene expression level analysis. First, the read count data was standardized by TMM (trimmed mean of M values)[16]. Then these genes were used for the different analysis. The thresholds are  $q\text{-value} < 0.005$  and  $|\log_2(\text{fold change})| > 1$ . For differential genes, if  $\log_2(\text{fold change}) > 0$  of the gene was greater than 0, the differential gene was considered to be up-regulated, whereas was considered to be down-regulated [40].

### **Differential gene GO function annotation, classification and KEGG analysis**

For GO (gene ontology) enrichment analysis, the gene ontology database of all DEGs was first mapped with each term to calculate the number of genes per term, and then significantly enriched in DEGs compared to the entire genome background [41].

KEGG (Kyoto encyclopedia of genes and genomes) is the main free database on Pathway. Pathway Significant enrichment analysis in the KEGG Pathway unit, a hypergeometric test was applied to get the path of differential genes that were significantly enriched relative to all annotated genes. Use KOBAS (2.0) (<http://kobas.cbi.pku.edu.cn>) and set the parameter FDR to BH (use Benjamini-Hochberg correction) [42] for Pathway enrichment analysis. Pathway with  $FDR \leq 0.05$ , called as a pathway that is significantly enriched in DEGs [43].

### **Physiological indexes**

The content of ATP was determined by spectrophotometric method according to the protocol of ATP kit (Comin Biotechnology Co., Ltd., Suzhou, China). Three ground C303A anther samples (0.1 g each) were placed in a centrifuge tube. Added 1 mL lysate and stirred well. The mixture was well homogenized for 10 min, centrifuged at 8000 r/min for 10 min at 4 °C, and the supernatant was taken to another centrifuge tube. Added 500 µL of chloroform and mixed well by shaking. Centrifuge at 10000 r/min for 3 min at 4 °C, take the supernatant, and place on ice for the ATP testing. And then through spectrophotometric method determined the content of ATP. In the same way, we measured the ATP content in the anther of 303B.

The contents of H<sub>2</sub>O<sub>2</sub>, O<sup>2-</sup> and MDA, as well as the CAT, POD and SOD activity levels were determined as described previously [44, 45].

### **Phylogenetic tree construction, characteristics conserved domain Structure and motif compositions analysis**

To identify all candidate MAD-box genes in our RNA-seq results, systematic BLASTp (<https://blast.ncbi.nlm.nih.gov/Blast.cgi>) searches were used to against the wheat reference genome ([https://plants.ensembl.org/Triticum\\_aestivum/Info/Index](https://plants.ensembl.org/Triticum_aestivum/Info/Index)) and the NCBI database and the screening criteria was E<1e-10 and protein length>200aa. The full-length amino acid sequences of MAD-box genes from maize (*Z. mays*), Arabidopsis (*A. thaliana*), and rice (*O. sativa*), were obtained from an online database (<https://www.ncbi.nlm.nih.gov/>) using NCBI BLASTp tools. Then using the maximum likelihood method [46] reconstruct the phylogenetic tree in MEGA6 (Molecular Evolutionary Genetics Analysis Version 6.0).

We submit all class B MADS-box genes protein sequences to MEME Suite web server (<http://meme-suite.org/>) for motif compositions analysis. The conserved domain were obtained from NCBI website (<https://www.ncbi.nlm.nih.gov/Structure/bwrpsb/bwrpsb.cgi>).

### **Real-time quantitative PCR (RT-qPCR) analysis**

Fifteen DEGs associated with fertility conversion correlation were randomly selected and Primer-NCBI (<https://www.ncbi.nlm.nih.gov/tools/primer-blast/>) designed primers (Table s3) were used for qRT-PCR analysis. RNA was reverse transcribed into cDNA by using the first strand cDNA synthesis kit (GeneStar Co.Ltd, Beijing, China), cDNA was used as a template, and Actin is used as internal ginseng. TaKaRa (Japan) SYBR® Premix Ex Taq™ II (Tli RNaseH Plus) kit was used. Fluorescence quantitative detection was performed on QuantStudio® 7 Flex Real-Time PCR system (Applied Biosystems, Shanghai, China). Three technical repetitions were performed for each sample, and the relative expression was assessed according to the 2<sup>-DDCt</sup> method [47].

## **Abbreviations**

CMS                      Cytoplasmic male sterility

DEGs	Differentially expressed genes
GO	Gene Ontology
KEGG	Kyoto Encyclopedia of Genes and Genomes
RNA-Seq	RNA sequencing technology
TDS	Tetrad stage,
EUNS	Early uninucleate stage
LUNS	Later uninucleate stage,
BNS	Binucleate stage,
TNS	trinucleate stage

## Declarations

### Ethics approval and consent to participate

This study does not contain any research requiring ethical consent of approval.

### Consent for Publication

Not applicable.

### Availability of data and material

All of datasets supporting the conclusions of this article are included within the article (and its additional files).

### Competing interests

The authors declare that they have no conflicts of interest

### Funding

This study was sponsored by the National Natural Science Foundation of China (31771874) and the Program in Science and Technology of Yangling State Demonstration Zone of Agricultural High-tech Industries (2018NY-19).

### Authors' contributions

XS and QL conceived and designed the study. QL performed the experiments, analyzed the data, and wrote the article with contributions from all of the authors. ZL and WL read and approved the manuscript.

## Acknowledgements

Not Applicable.

## References

1. Paux E, Sourdille P, Salse J, Saintenac C, Choulet F, Leroy P, Korol A, Michalak M, Kianian S, Spielmeyer W *et al.* **A physical map of the 1-gigabase bread wheat chromosome 3B.** *Science (New York, NY)* 2008, **322**(5898):101-104.
2. Singh RP, Singh PK, Rutkoski J, Hodson DP, He X, Jorgensen LN, Hovmoller MS, Huerta-Espino J: **Disease Impact on Wheat Yield Potential and Prospects of Genetic Control.** *Annual review of phytopathology* 2016, **54**:303-322.
3. Gao F, Ma D, Yin G, Rasheed A, Dong Y, Xiao Y, Xia X, Wu X, He Z: **Genetic Progress in Grain Yield and Physiological Traits in Chinese Wheat Cultivars of Southern Yellow and Huai Valley since 1950.** *Crop Science* 2017, **57**(2):760-773.
4. Zhang G, Ye J, Jia Y, Zhang L, Song X: **iTRAQ-Based Proteomics Analyses of Sterile/Fertile Anthers from a Thermo-Sensitive Cytoplasmic Male-Sterile Wheat with *Aegilops kotschyi* Cytoplasm.** *International journal of molecular sciences* 2018, **19**(5).
5. Chen L, Liu YG: **Male sterility and fertility restoration in crops.** *Annual review of plant biology* 2014, **65**:579-606.
6. Murai K, Tsunewaki K: **Photoperiod-sensitive cytoplasmic male sterility in wheat with *Aegilops crassa* cytoplasm.** *Euphytica* 1993, **67**(1):41-48.
7. Saraïke T, Shitsukawa N, Yamamoto Y, Hagita H, Iwasaki Y, Takumi S, Murai K: **Identification of a protein kinase gene associated with pistillody, homeotic transformation of stamens into pistil-like structures, in alloplasmic wheat.** *Planta* 2007, **227**(1):211-221.
8. Coen ES, Meyerowitz EM: **The war of the whorls: genetic interactions controlling flower development.** *Nature* 1991, **353**(6339):31-37.
9. Pelaz S, Ditta GS, Baumann E, Wisman E, Yanofsky MF: **B and C floral organ identity functions require SEPALLATA MADS-box genes.** *Nature* 2000, **405**(6783):200-203.
10. Theissen G: **Development of floral organ identity: stories from the MADS house.** *Current opinion in plant biology* 2001, **4**(1):75-85.
11. Hama E, Takumi S, Ogihara Y, Murai K: **Pistillody is caused by alterations to the class-B MADS-box gene expression pattern in alloplasmic wheats.** *Planta* 2004, **218**(5):712-720.
12. Goto K, Meyerowitz EM: **Function and regulation of the Arabidopsis floral homeotic gene PISTILLATA.** *Genes & development* 1994, **8**(13):1548-1560.
13. Trobner W, Ramirez L, Motte P, Hue I, Huijser P, Lonig WE, Saedler H, Sommer H, Schwarz-Sommer Z: **GLOBOSA: a homeotic gene which interacts with DEFICIENS in the control of *Antirrhinum* floral organogenesis.** *The EMBO journal* 1992, **11**(13):4693-4704.

14. Ye J, Fang L, Zheng H, Zhang Y, Chen J, Zhang Z, Wang J, Li S, Li R, Bolund L *et al*: **WEGO: a web tool for plotting GO annotations.** *Nucleic acids research* 2006, **34**(Web Server issue):W293-297.
15. Li J, Ding X, Han S, He T, Zhang H, Yang L, Yang S, Gai J: **Differential proteomics analysis to identify proteins and pathways associated with male sterility of soybean using iTRAQ-based strategy.** *Journal of proteomics* 2016, **138**:72-82.
16. Liu Z, Shi X, Li S, Zhang L, Song X: **Oxidative Stress and Aberrant Programmed Cell Death Are Associated With Pollen Abortion in Isonuclear Alloplasmic Male-Sterile Wheat.** *Frontiers in plant science* 2018, **9**:595.
17. Geng X, Ye J, Yang X, Li S, Zhang L, Song X: **Identification of Proteins Involved in Carbohydrate Metabolism and Energy Metabolism Pathways and Their Regulation of Cytoplasmic Male Sterility in Wheat.** *International journal of molecular sciences* 2018, **19**(2).
18. Song.Xiyue, Yingang H, lingjian M: **Changes of material content in panicles and leaves of YS type thermo-sensitive male sterile wheat line A3314 during transfer from sterility to fertility.** *Journal of Northwest A &F University* 2009, **37**(8):81-86.
19. Xianliang S, Xuezhen S, honggang W: **Biochemical changes in anthers of "Dong A" genetic male sterile lines of cotton.** *Acta Botanica Boreali-Occidentalia Sinica* 2004, **24**(2):243-247.
20. Tang XJ, Peng C, Zhang J, Cai Y, You XM, Kong F, Yan HG, Wang GX, Wang L, Jin J *et al*: **ADP-glucose pyrophosphorylase large subunit 2 is essential for storage substance accumulation and subunit interactions in rice endosperm.** *Plant science : an international journal of experimental plant biology* 2016, **249**:70-83.
21. Kang GZ, Wang YH, Liu C, Shen BQ, Zheng BB, Feng W, Guo TC: **Difference in AGPase subunits could be associated with starch accumulation in grains between two wheat cultivars.** *Plant Growth Regulation* 2010, **61**(1):61-66.
22. Cheng C, Hu J, Zhi Y, Su JJ, Zhang XK, Huang BQ: **Cloning and characterization of ADP-glucose pyrophosphorylase small subunit gene in *Cyperus esculentus* (yellow nutsedge).** *Genetics and molecular research : GMR* 2015, **14**(4):18302-18314.
23. Li J, Pandeya D, Jo YD, Liu WY, Kang BC: **Reduced activity of ATP synthase in mitochondria causes cytoplasmic male sterility in chili pepper.** *Planta* 2013, **237**(4):1097-1109.
24. Tao X, Jilin L: **Cytochrome Oxidase Activity and ATP Content of Male-Sterile Cytoplasm in Maize(*Zea mays* L.).** *Journal of north China agriculture* 1994, **9**(4):33-37.
25. Jack T, Brockman LL, Meyerowitz EM: **The homeotic gene APETALA3 of *Arabidopsis thaliana* encodes a MADS box and is expressed in petals and stamens.** *Cell* 1992, **68**(4):683-697.
26. Sommer H, Beltran JP, Huijser P, Pape H, Lonig W, Saedler H, Schwarz-Sommer Z: **Deficiens, a homeotic gene involved in the control of flower morphogenesis in *Antirrhinum majus*: the protein shows homology to transcription factors.** *The EMBO journal* 1990, **9**(3):605-613.
27. McGonigle B, Bouhidel K, Irish VF: **Nuclear localization of the *Arabidopsis* APETALA3 and PISTILLATA homeotic gene products depends on their simultaneous expression.** *Genes & development* 1996, **10**(14):1812-1821.

28. E H, S T, Y O, K M: **Pistillody is caused by alterations to the class-B MADS-box gene expression pattern in alloplasmic wheats.** *Planta* 2004, **218**(5):712-720.
29. Mizzotti C, Mendes MA, Caporali E, Schnittger A, Kater MM, Battaglia R, Colombo L: **The MADS box genes SEEDSTICK and ARABIDOPSIS Bsister play a maternal role in fertilization and seed development.** *The Plant journal : for cell and molecular biology* 2012, **70**(3):409-420.
30. Kang HG, Jeon JS, Lee S, An G: **Identification of class B and class C floral organ identity genes from rice plants.** *Plant molecular biology* 1998, **38**(6):1021-1029.
31. Becker A, Theissen G: **The major clades of MADS-box genes and their role in the development and evolution of flowering plants.** *Molecular phylogenetics and evolution* 2003, **29**(3):464-489.
32. Paolacci AR, Tanzarella OA, Porceddu E, Varotto S, Ciaffi M: **Molecular and phylogenetic analysis of MADS-box genes of MIKC type and chromosome location of SEP-like genes in wheat (*Triticum aestivum* L.).** *Molecular genetics and genomics : MGG* 2007, **278**(6):689-708.
33. Pinyopich A, Ditta GS, Savidge B, Liljegren SJ, Baumann E, Wisman E, Yanofsky MF: **Assessing the redundancy of MADS-box genes during carpel and ovule development.** *Nature* 2003, **424**(6944):85-88.
34. Zhou LL, Song GQ, Hong-Yan LI, Yin-Gang HU, Bei-Ru, He: **A MADS-Box Transcription Factor Related to Fertility Conversion in Male Sterile Wheat Lines.** *Acta Agronomica Sinica* 2008, **34**(4):598-604.
35. Sun Q, Qu J, Yu Y, Yang Z, Wei S, Wu Y, Yang J, Peng Z: **TaEPFL1, an EPIDERMAL PATTERNING FACTOR-LIKE (EPFL) secreted peptide gene, is required for stamen development in wheat.** *Genetica* 2019, **147**(2):121-130.
36. Liu Z, Shi X, Zhang L, Song X: **Tapetal Programmed Cell Death, Antioxidant Response and Oxidative Stress in Wheat Anthers Associated with D 2 -type Cytoplasmic Male-Sterility.** *Scientia Agricultura Sinica* 2017, **50**(21):4071-4086.
37. Wang S, Zhang G, Song Q, Zhang Y, Li Z, Guo J, Niu N, Ma S, Wang J: **Abnormal development of tapetum and microspores induced by chemical hybridization agent SQ-1 in wheat.** *PloS one* 2015, **10**(3):e0119557.
38. Roberts A, Pimentel H, Trapnell C, Pachter L: **Identification of novel transcripts in annotated genomes using RNA-Seq.** *Bioinformatics (Oxford, England)* 2011, **27**(17):2325-2329.
39. Zararsiz G, Cosgun E: **Introduction to statistical methods for microRNA analysis.** *Methods in molecular biology (Clifton, NJ)* 2014, **1107**:129-155.
40. Wang L, Feng Z, Wang X, Wang X, Zhang X: **DEGseq: an R package for identifying differentially expressed genes from RNA-seq data.** *Bioinformatics (Oxford, England)* 2010, **26**(1):136-138.
41. Young MD, Wakefield MJ, Smyth GK, Oshlack A: **Gene ontology analysis for RNA-seq: accounting for selection bias.** *Genome biology* 2010, **11**(2):R14.
42. Benjamini Y, Hochberg Y: **Controlling The False Discovery Rate - A Practical And Powerful Approach To Multiple Testing.** *Journal of the Royal Statistical Society* 1995, **57**(1):289-300.

43. Kanehisa M, Araki M, Goto S, Hattori M, Hirakawa M, Itoh M, Katayama T, Kawashima S, Okuda S, Tokimatsu T *et al*: **KEGG for linking genomes to life and the environment**. *Nucleic acids research* 2008, **36**(Database issue):D480-484.
44. Ba QS, Zhang GS, Wang JS, Che HX, Liu HZ, Niu N, Ma SC, Wang JW: **Relationship between metabolism of reactive oxygen species and chemically induced male sterility in wheat (*Triticum aestivum* L.)**. *Canadian Journal of Plant Science* 2013, **93**(4):675-681.
45. Jacoby RP, Millar AH, Taylor NL: **Wheat mitochondrial proteomes provide new links between antioxidant defense and plant salinity tolerance**. *Journal of proteome research* 2010, **9**(12):6595-6604.
46. Tamura K, Stecher G, Peterson D, Filipski A, Kumar S: **MEGA6: Molecular Evolutionary Genetics Analysis version 6.0**. *Molecular biology and evolution* 2013, **30**(12):2725-2729.
47. Lim S, Yoon H, Ryu S, Jung J, Lee M, Kim D: **A comparative evaluation of radiation-induced DNA damage using real-time PCR: influence of base composition**. *Radiation research* 2006, **165**(4):430-437.

## Tables

**Table 1.** Differentially abundant proteins related to starch and sucrose metabolism in fertile and sterile plants.

## Additional Files

**Additional file1** **table s1.** B706-vs-C706A GO Enrichment in Biological Process.

**Additional file2** **table s2.** B706-vs-C706A Pathway Enrichment .

**Additional file3** **table s3.** Phylogenetic tree of MADS-box transcription factor genes in different plant species.

**Additional file4** **table s4.** Sequence-specific primers used for qRT-PCR.

Additional file5 figure s1. the results of amino acid sequence alignment of TaAG114 and OsMADS32.

Additional file6 figure s2. the results of amino acid sequence alignment of WM25 and OsMADS29.

## Figures



Figure 1

Morphology of 303B (A, C, E) and C303A (B, D, F) plants. (A, B) Inflorescence of 303B and C303A, showing stamen. (C, D) Microspore of I2 -KI staining. (E, F) morphology of 303B and C303A stamen. Scale bars are 50  $\mu$ m (C, D), and 200  $\mu$ m (E, F).

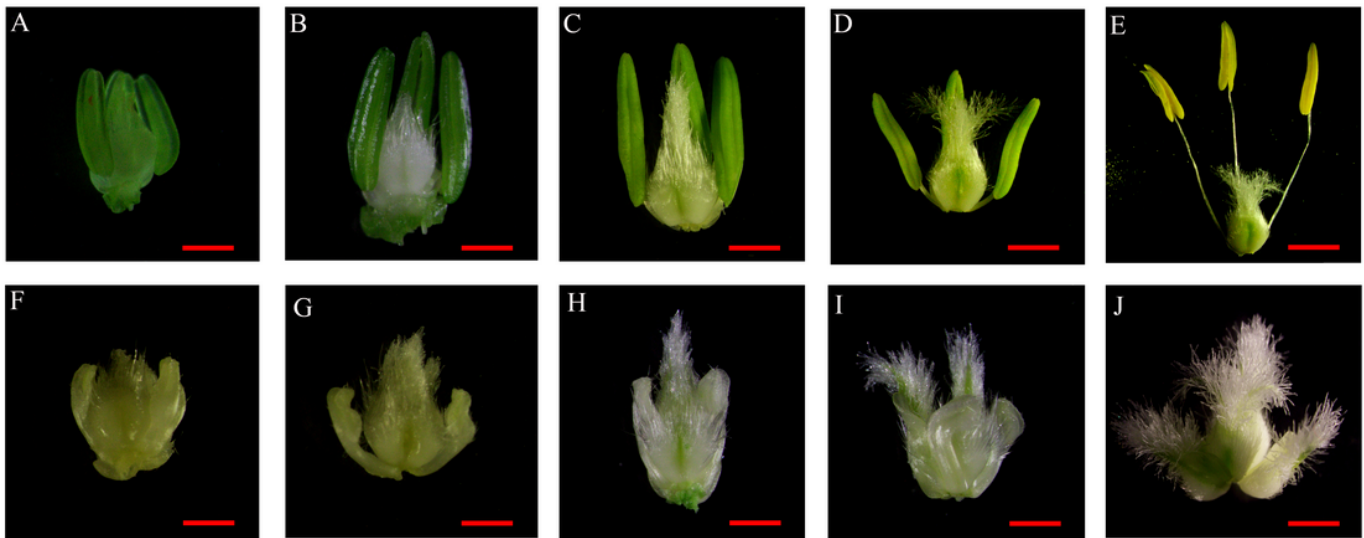


Figure 2

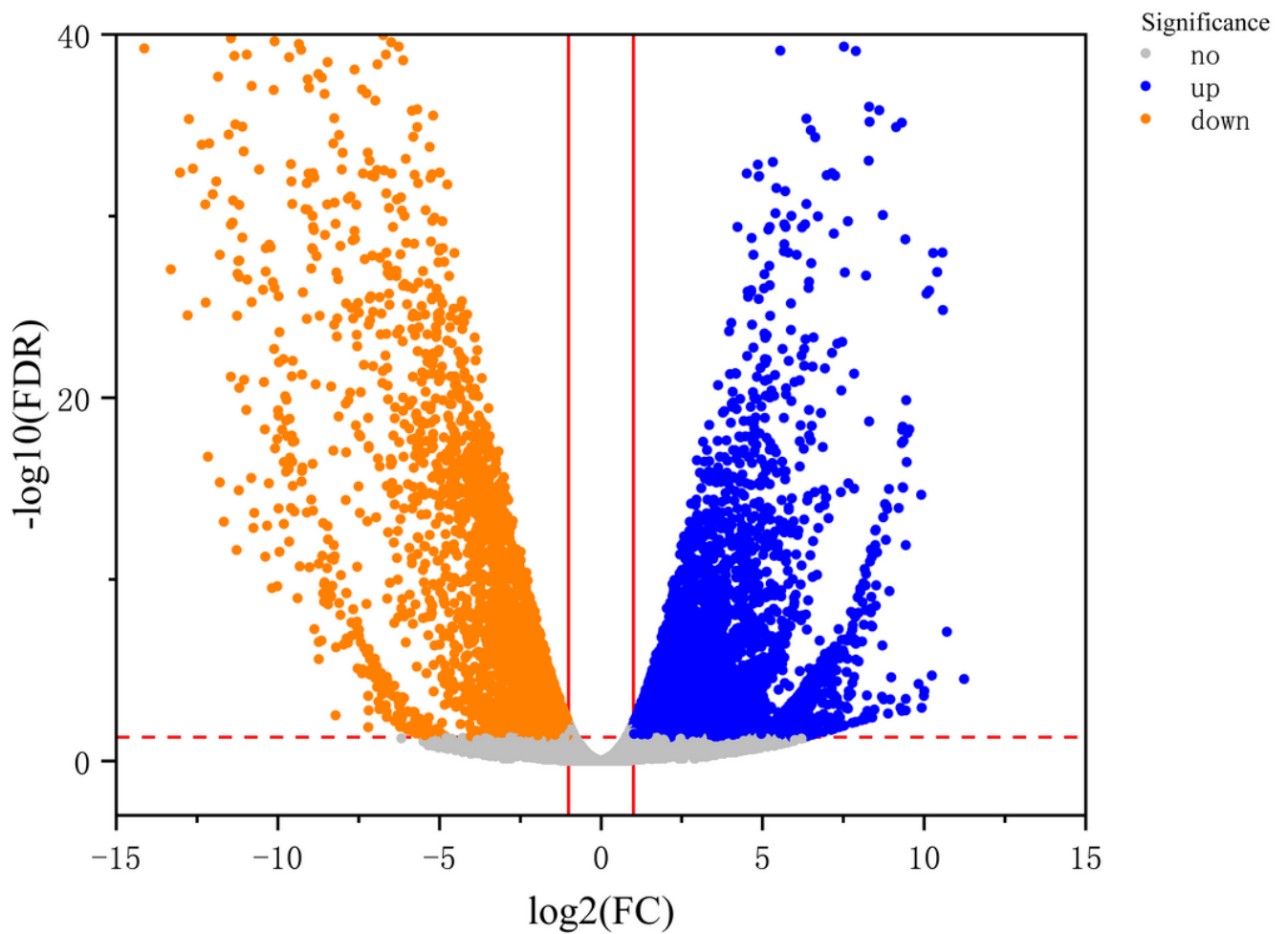
Comparisons of the anther phenotype in 303B (A-E) and C303A (F-J). (A, F) TDS, tetrad stage; (B, G) EUNS, early uninucleate stage; (C, H) LUNS, late uninucleate stage; (D, I) BNS, binucleate stage; and (E, J) TNS, trinucleate stage. Scale bars are 1 mm in (A–J).



Figure 3

Transverse and longitudinal sections of normal stamen and pistil-like stamen. Transverse section of normal stamens from 303B (A-E) and pistil-like stamens from C303A (F-J). Comparisons of anther locule in 303B and C303A during difference stages. Longitudinal section of normal stamens from 303B (A2-E2) and pistil-like stamens from C303A (F2-J2). E: Epidermis; En: Endothecium; ML: Middle layer; T: Tapetum;

Msp: Microspores. V: vascular bundle, Ov: ovule. Scale bars are 100  $\mu\text{m}$  in (A-I, J1 ), 50 $\mu\text{m}$  (A1-I1), and 200  $\mu\text{m}$ (A2-J2,J).



**Figure 4**

Comparison of gene expression levels of every gene in C303A relative to 303B at the binucleate stage. Gray dots indicate no significant difference sense, the blue dots indicate significantly up-regulated genes, the orange dots indicate significantly down regulated genes.

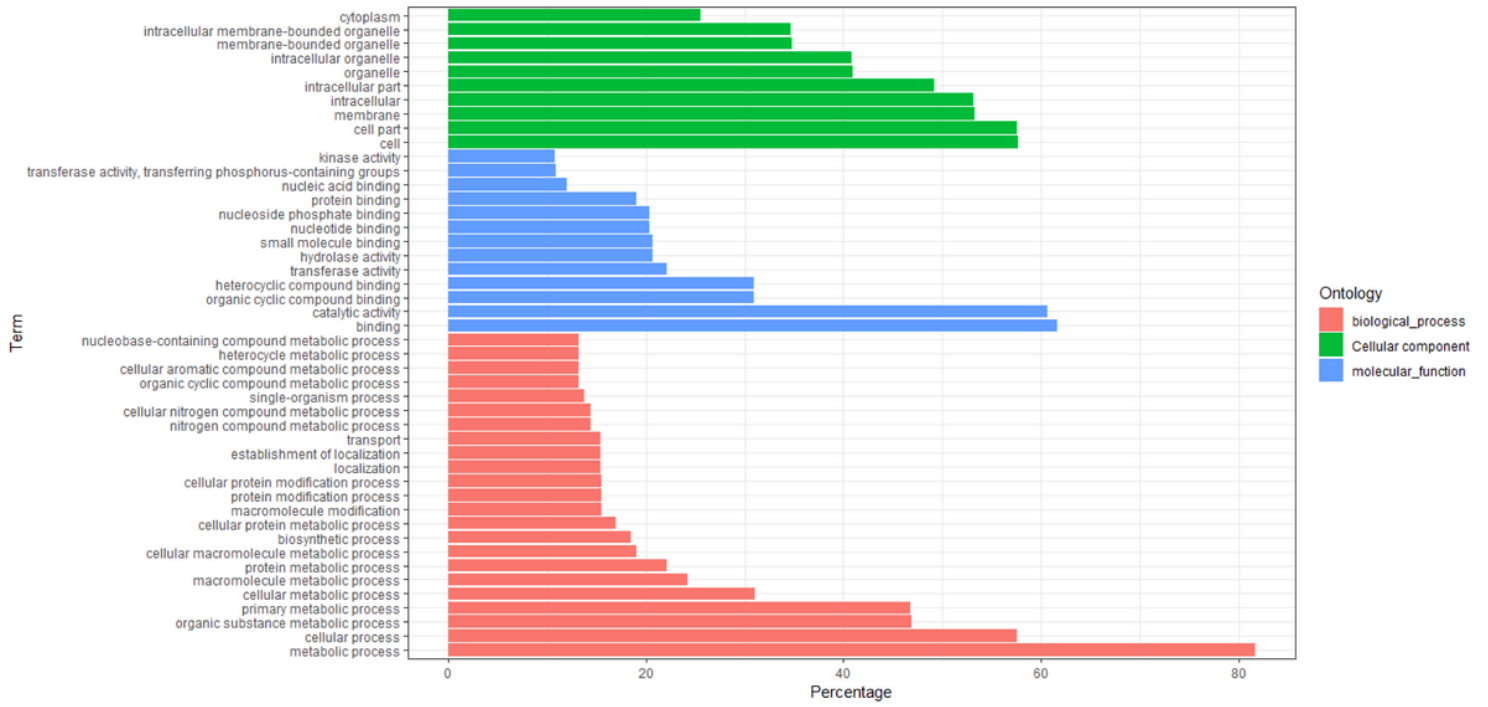


**Figure 5**

Gene Ontology (GO) classifications of differentially expression genes (DEGs) in C303A and 303B at the binucleate stage.

Pathway

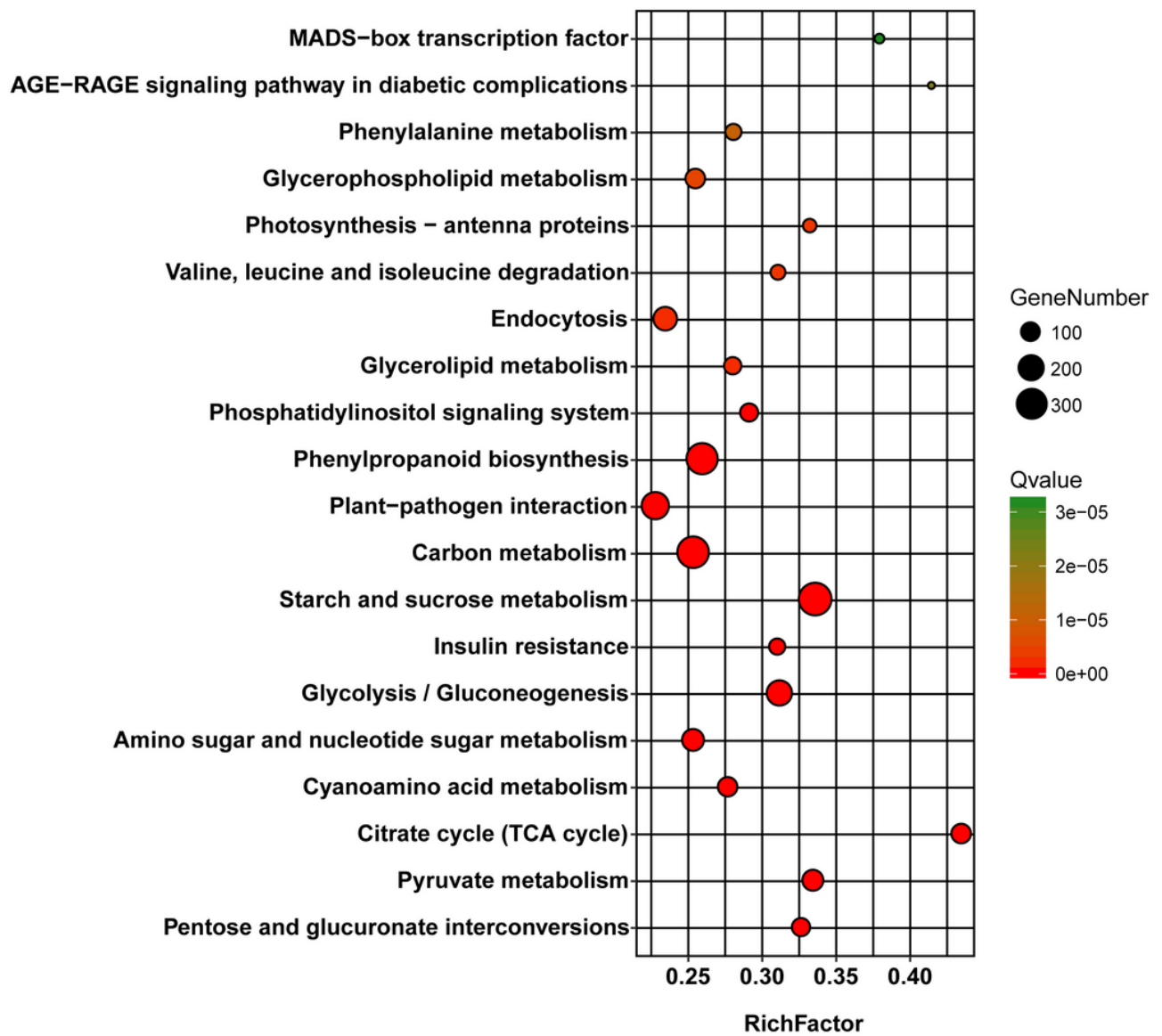
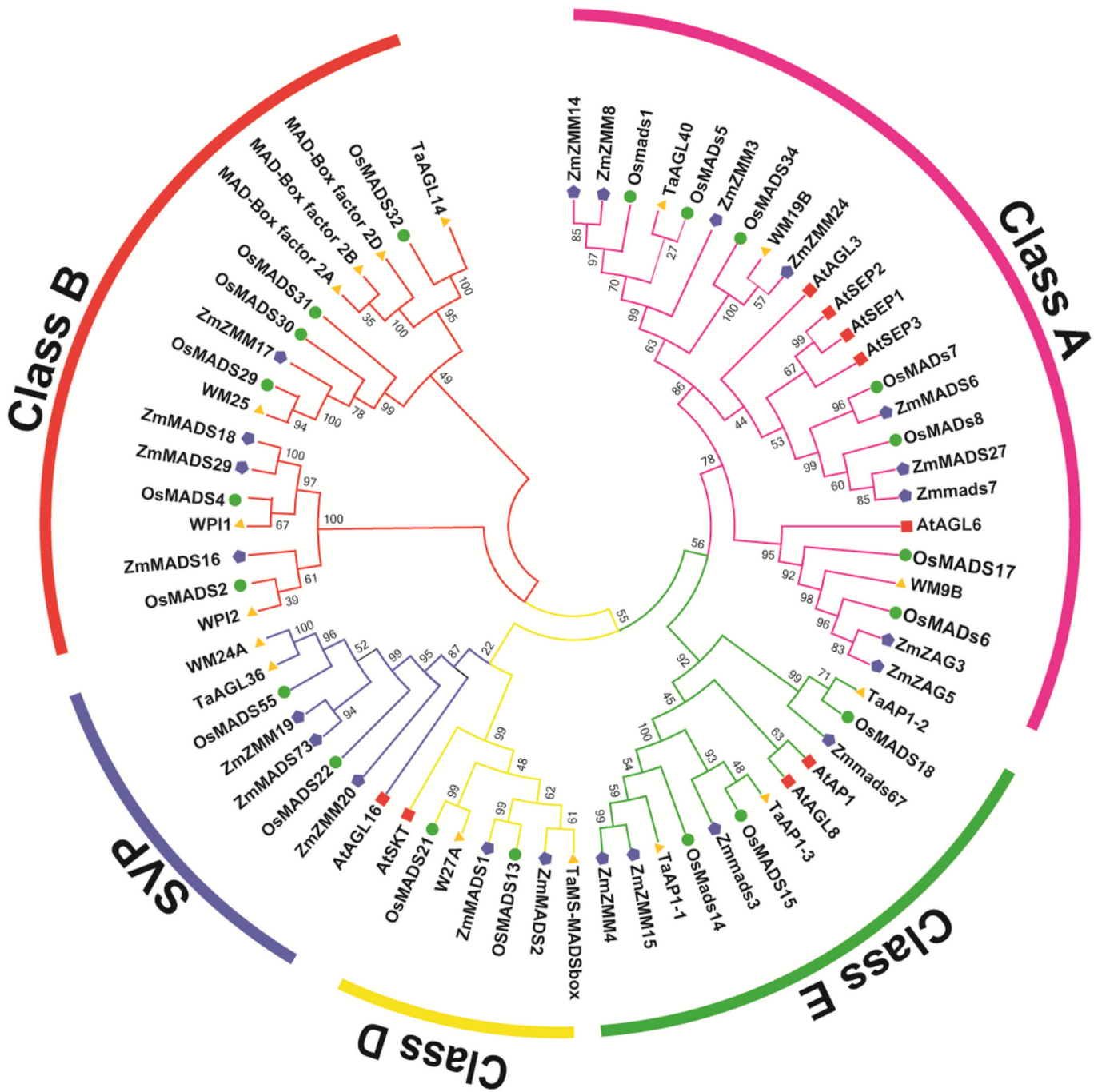


Figure 6

Top 20 significant enrichment pathways. Large RichFactor indicates a high degree of enrichment.



**Figure 7**

Phylogenetic tree of MADS-box transcription factor genes in different plant species. The full-length amino acid sequences of MADS-box transcription factor genes from maize (*Z. mays*), Arabidopsis (*A. thaliana*), rice (*O. sativa*) and wheat (*Triticum aestivum* L) were obtained from online NCBI database. The phylogenetic trees were constructed using the MEGA 6.0. (The detailed information of these genes can be seen in Supplementary TableS4.)

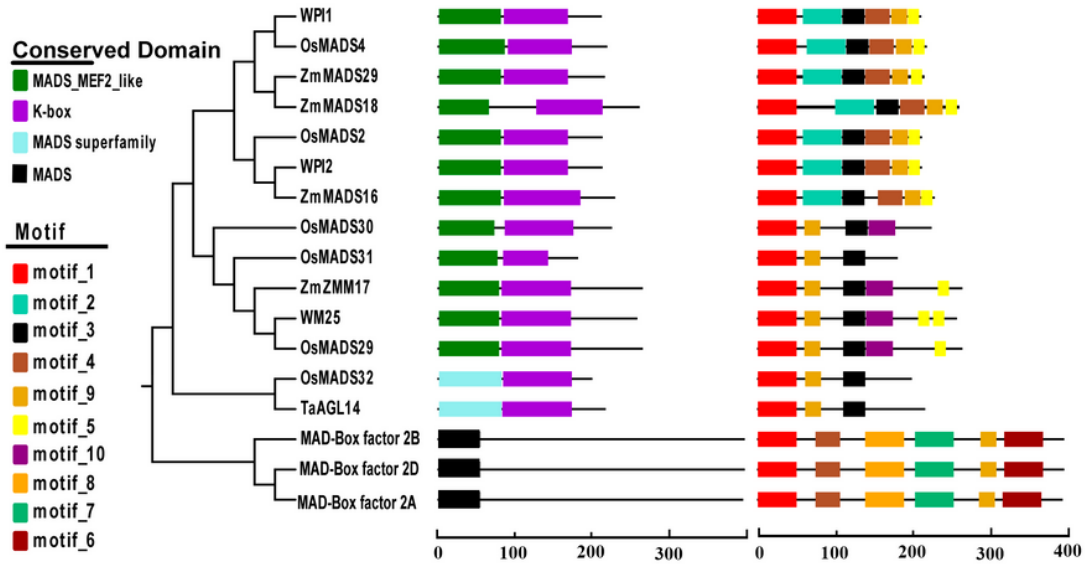


Figure 8

.Phylogenetic relationships conserved domain and motif compositions of class B MAD-box genes.

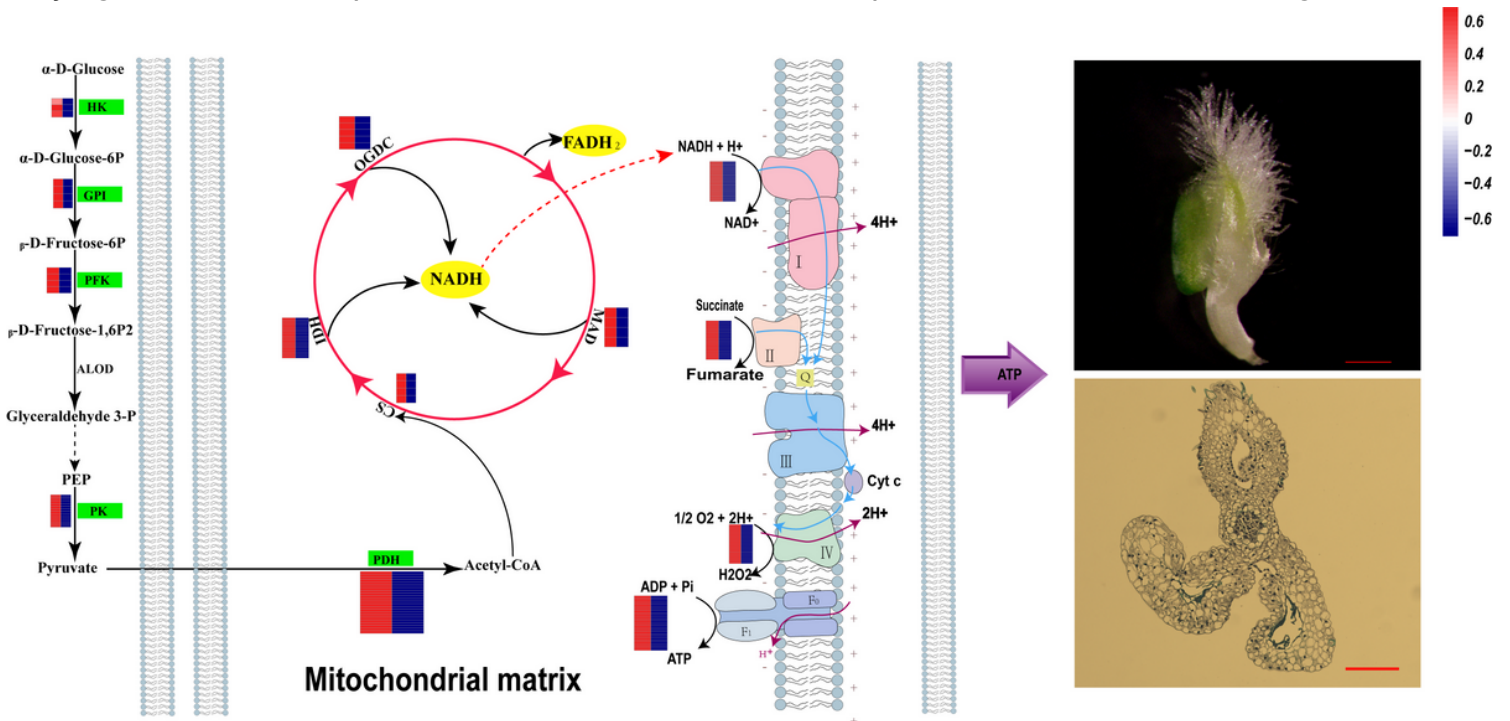


Figure 9

Possible genes network responsible for controlling no microspores in wheat. HK: hexokinase; GPI: glucose-6-phosphate isomerase; PFK: 6-phosphofructokinase1; ALDO: fructose-bisphosphate aldolase;

PK: pyruvate kinase; PDH: Pyruvate dehydrogenase; CS: citrate synthase; IDH, isocitrate dehydrogenase; OGDC: 2-oxoglutarate dehydrogenase, MAD: Malate dehydrogenase; NADH dehydrogenase; II: succinate dehydrogenase; IV: Cytochrome c oxidase. V: ATP synthase; The left side represents 303B and the right side represents C303A in the heatmap.

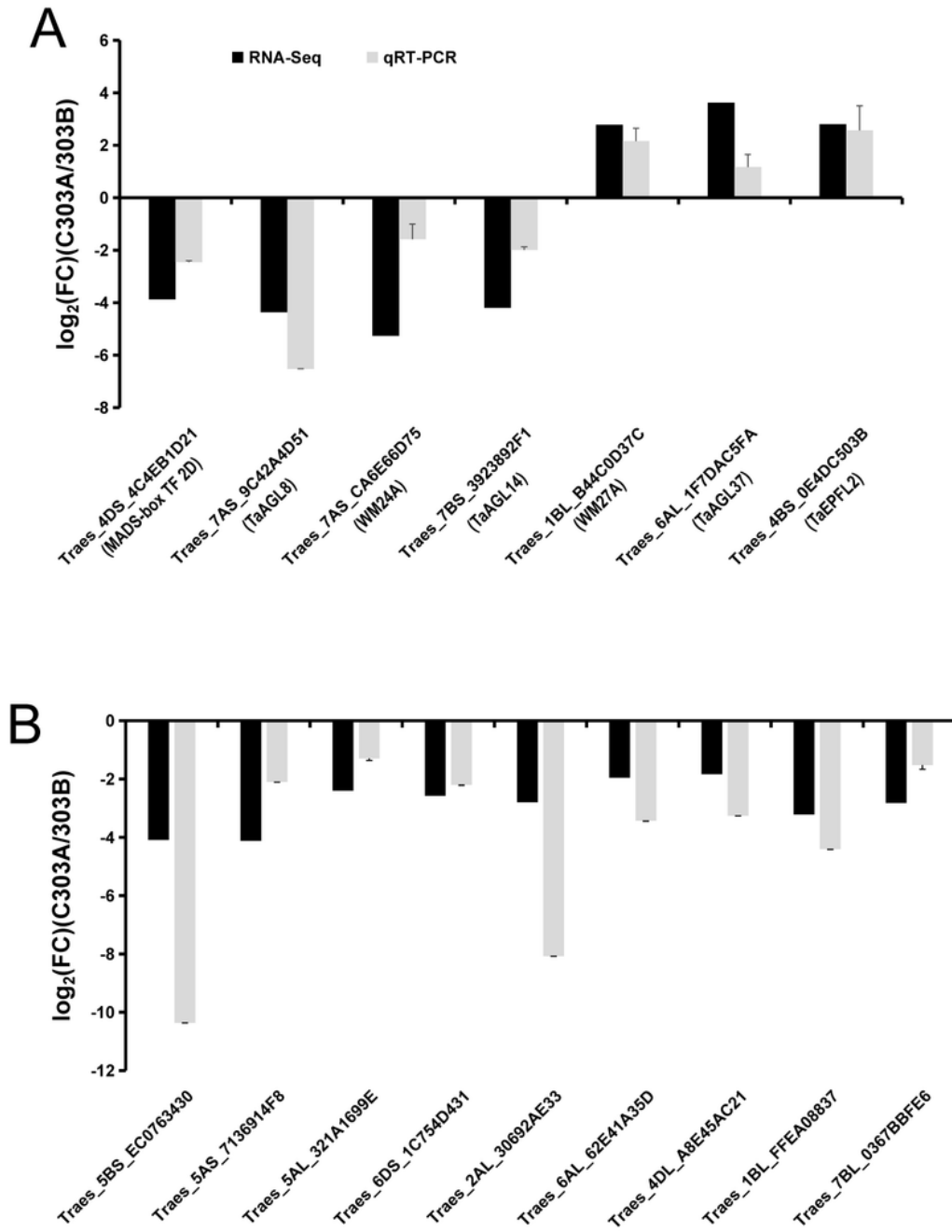
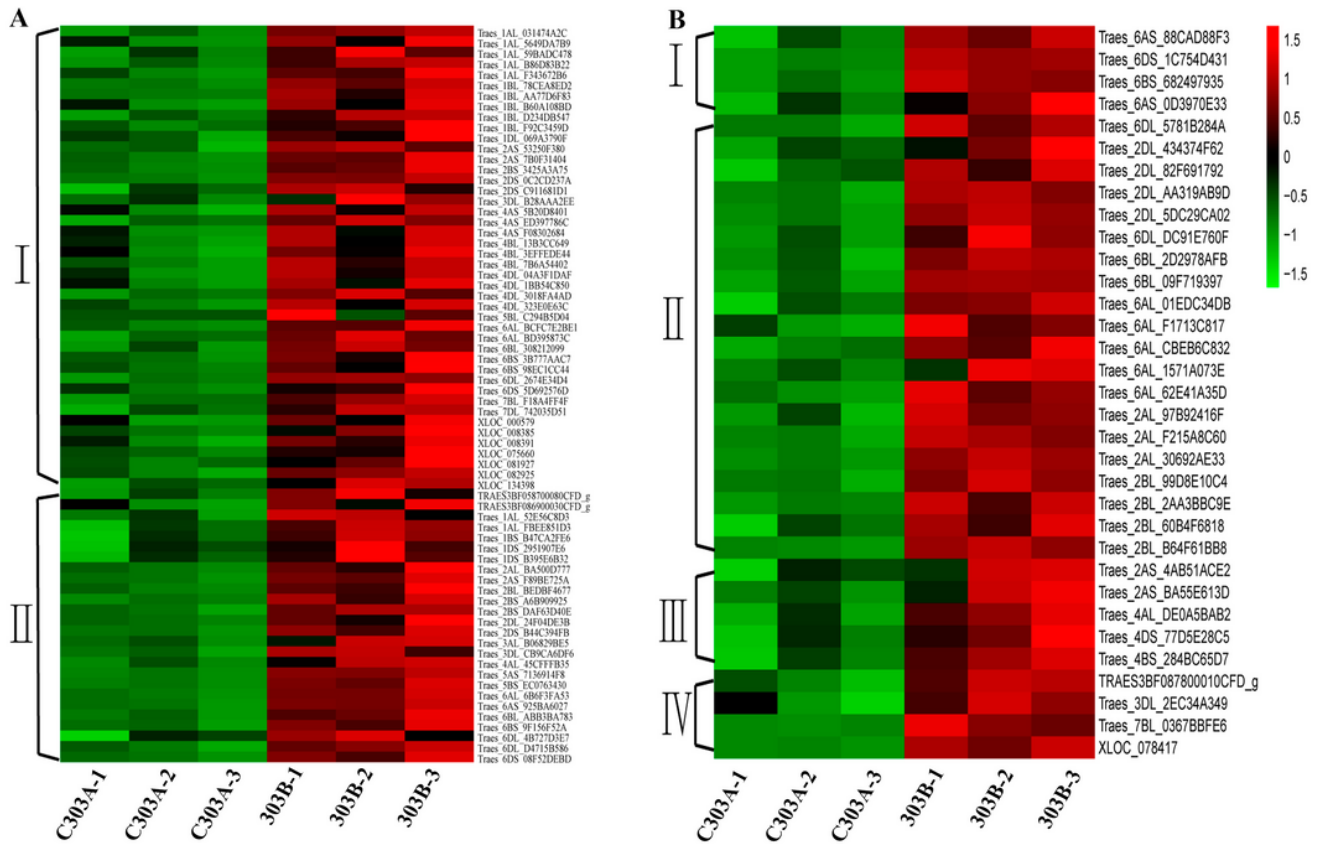


Figure 10

qRT-PCR validates the RNA sequencing result of some DEGs. Log2 (FC) represents logarithmic value of change in expression for C303A relative to 303B. DEGS related to Pistillody (A) and involved in the process of energy metabolism (B).



**Figure 11**

Hierarchical clustering analysis of differentially expression genes (DEGs) with energy metabolism pathway at binucleate stage. (A) DEGs involved in ETC, including NADH dehydrogenase (A-I), ATP synthase (A-II). (B) DEGS involved incitric acid cycle, including Citrate synthase (B-I), Isocitrate dehydrogenase (B-II), 2-oxoglutarate dehydrogenase (B-III) and Malate dehydrogenase (B-IV).

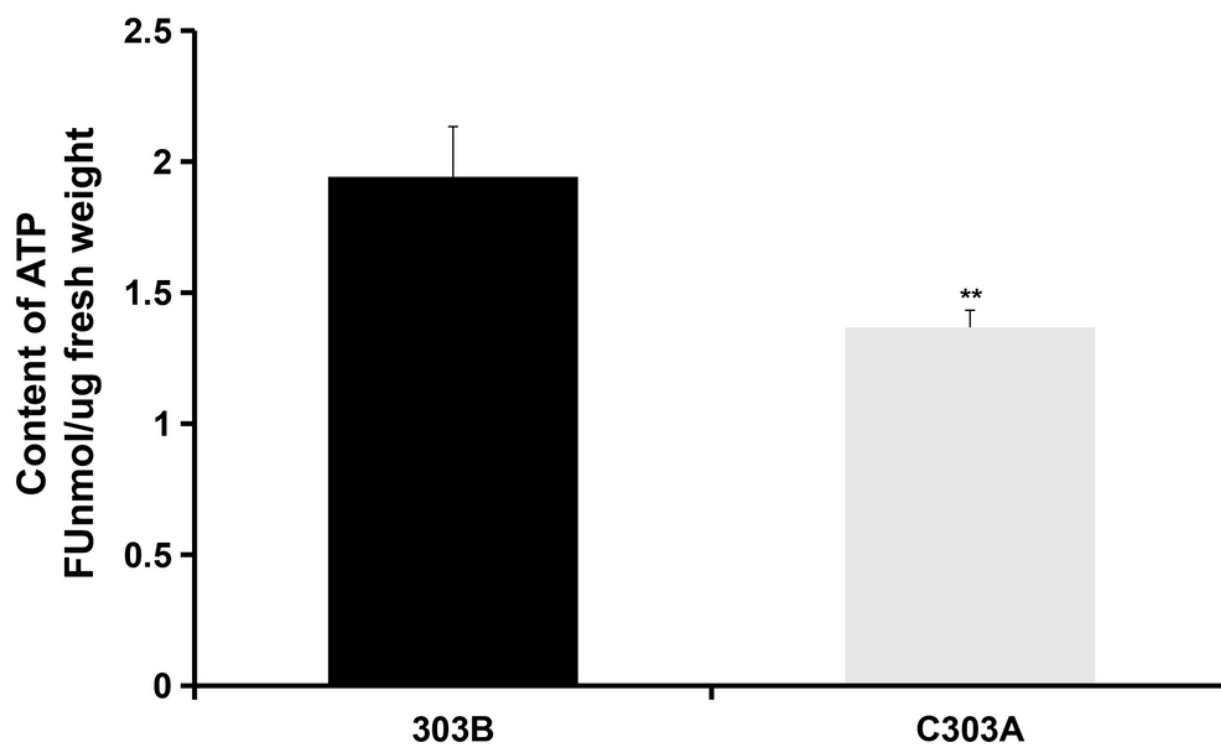
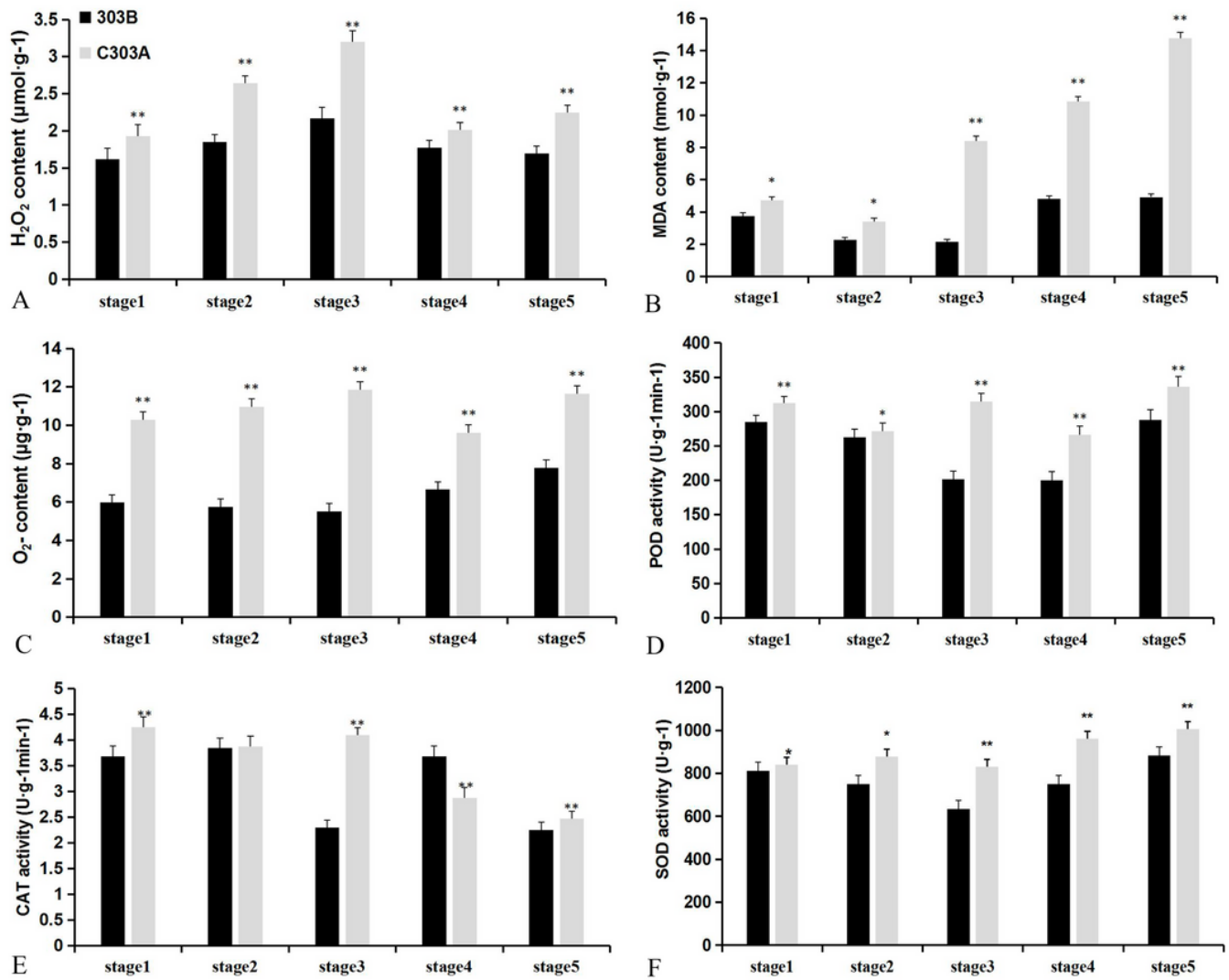


Figure 12

ATP content of stamen from the maintainer line 303B and sterile line C303A during BNS stage. Data represent the mean and standard deviation based on three replicates. \*\*  $p < 0.01$ .



**Figure 13**

The H<sub>2</sub>O<sub>2</sub> production rate (A), MDA (B) and O<sub>2</sub><sup>-</sup> (C) contents and activities of peroxidase (POD) (D), catalase (CAT) (E) and superoxide dismutase (SOD) (F) in developing stamen. Data represent the mean and standard deviation based on three replicates. (\*\* p < 0.01, \* p < 0.05).

## Supplementary Files

This is a list of supplementary files associated with this preprint. Click to download.

- [supplement1.emf](#)
- [supplement2.xlsx](#)
- [supplement3.xlsx](#)
- [supplement4.xlsx](#)
- [supplement5.xlsx](#)

- [supplement6.emf](#)
- [supplement7.xlsx](#)